Comparison of Spark Plasma Sintering and Hybrid Spark Plasma Sintering of Ni-Fe Alloys

Mxolisi B. Shongwe, Munyadziwa M. Ramakokovhu, Moipane L. Lethabane and Peter A. Olubambi

***Abstract*— Mixed Ni-50%Fe powders were sintered via spark plasma sintering (SPS) and hybrid spark plasma sintering (HSPS) techniques with 30 mm and 60 mm samples in both conditions. After SPS and HSPS, the 30 mm and 60 mm alloys (except 60mm-SPS) had a relative density (>99.0%) close to the theoretical density. Phase, microstructure and mechanical properties evolution of Ni-50%Fe alloy during SPS and HSPS were studied. The microstructural evolution of the 60 mm alloys varied from the edge of the sample to the core of the sample. Results show that the grain size and the hardness vary considerable from the edge to the core of sintered sample of 60 mm sintered using conventional SPS compared to hybrid SPS. Similarly, the hardness also increased from the edge to the core.**

***Index Terms*—Spark plasma sintering, Microstructure, Hardness, Fracture**

I. Introduction

Novel materials, such as advanced ferritic and austenitic steels, Ni-based superalloys and thermal barrier coatings, have contributed significantly to increase the efficiency of fossil-fueled power plants for reducing the emission of greenhouse gases and improving energy conservation [1-5]. Current developments on the Ni-Fe-based austenitic matrix which falls under the class of Ni-based alloy are encouraging to materials researchers due to their low cost and better workability, however it is important to note that this alloy are mainly fabricated via vacuum induction melting [6]. Unfortunately, to the best of our knowledge, work on these Ni-based alloy fabricated by spark plasma sintering (SPS) system has been rarely reported.

Mxolisi B. Shongwe is with the Institute for NanoEngineering Research, Department of Chemical, Metallurgical and Materials Engineering, Tshwane University of Technology, Pretoria, South Africa (email: m.shonwgem@gmail.com)

Munyadziwa M. Ramakokovhu is with the Institute for NanoEngineering Research, Department of Chemical, Metallurgical and Materials Engineering, Tshwane University of Technology, Pretoria, South Africa (Email: RamakokovhuM@tut.ac.za)

Moipone L. Lethabane is with the Institute for NanoEngineering Research, Department of Chemical, Metallurgical and Materials Engineering, Tshwane University of Technology, Pretoria, South Africa (LethabaneL@tut.ac.za)

Peter A. Olubambi is with the Department of Chemical Engineering Technology, University of Johannesburg, Johannesburg, South Africa (polubambi@gmail.com)

The financial assistance of the Department of Higher Education and Training [DHET] funding under the Tshwane University of Technology, Emerging Program Grant. This work is based on the research supported in part by the National Research Foundation of South Africa for the grant, Unique Grant No. 99348.

SPS, often referred to as field assisted sintering technique (FAST) or pulsed electric current sintering (PECS), is a newly arising sintering technique that employs a pulsed direct current (DC) to powders subjected to a modest applied pressure (<100 MPa). High electrical current application enables a fast heating rate (up to 1000 °C.min^{-1}), resulting in a very short sintering cycle, typically a few minutes for full densification of both conductive and nonconductive powders [7,8]. In such a case, a high densification rate is favoured whereas coarsening induced by surface diffusion is minimized, and then grain growth can be suppressed. Moreover, it is stated that SPS can offer other benefits, such as partial oxide film elimination, adsorbed gas release and surface activation of powder particles [9,10]. Recently, the SPS technique has been successfully used to prepare Fe-Ni alloys [11,12]. These features elevate the potential of SPS for wide spread application and comprehensive research in the field of materials.

Most spark plasma sintered samples investigated by some researchers are cylindrical with 20 mm diameter [13,14]. Such a small size could present difficulties in preparing suitable samples for measuring physical properties, such as tensile properties. Even more importantly, in real life applications, for national defence [15], aviation, and civil industries [16], much larger materials are required for these applications in the case of materials fabricated using the sintering method. Preparing much larger samples (>40 mm diameter) presents a difficulty when using SPS in getting homogenous properties within the samples due to poor heat distribution as the sample size gets bigger. Although, the SPS method has several advantages that distinguish it from the traditional sintering methods such as hot pressing and sintering of pre-compacted billets without pressure. Certain disadvantages of the standard SPS/FAST technology are observed (Fig. 1(a)), especially when sintering bigger samples, such as radial thermal gradient by thermal drain to the outside or non-heating of the material by too low electrical conductivity. Radial thermal gradient results in inhomogeneous radial microstructures. In the new hybrid spark plasma sintering system (HHPD-25 from FCT Sytem GmbH Germany) radial thermal gradient are eliminated, as the material can be heated additionally and/or exclusively by induction/resistance heating beside heating by pulsed direct current passage (Fig. 1(b)) [17]. Significant increase of sintering activity for certain materials by hybrid heating (combination of SPS/FAST technology +

ISBN: 978-988-14048-3-1
ISSN: 2078-0958 (Print); ISSN: 2078-0966 (Online)

resistance/induction heating) could be proved offering homogeneous radial densification. This will result in considerably shorter cycle time and production time. Considering that this is a new technology, Ni-Fe alloys fabricated by this technology has not been reported in the literature, including the advantages offered by this new technology when fabricating samples larger than 40mm. Thus, the mechanical properties and microstructural evolution of Ni-50%Fe alloys sintered by the standard SPS/FAST technology compared to those sintered by the hybrid technology will be investigated in this paper.

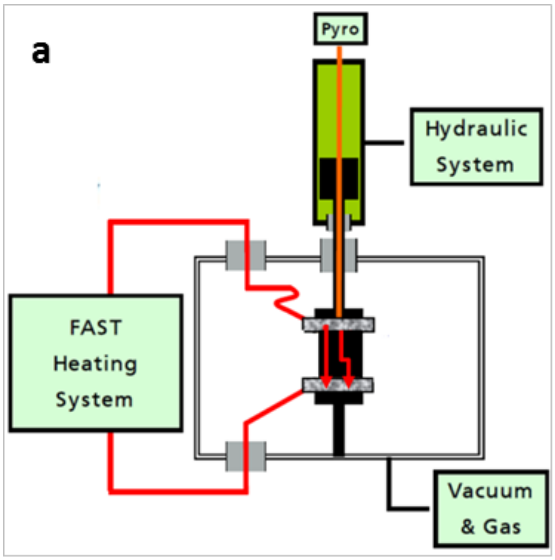

Fig. 1 (a) Schematic of the Spark Plasma Sintering apparatus: standard SPS/FAST technology [17].

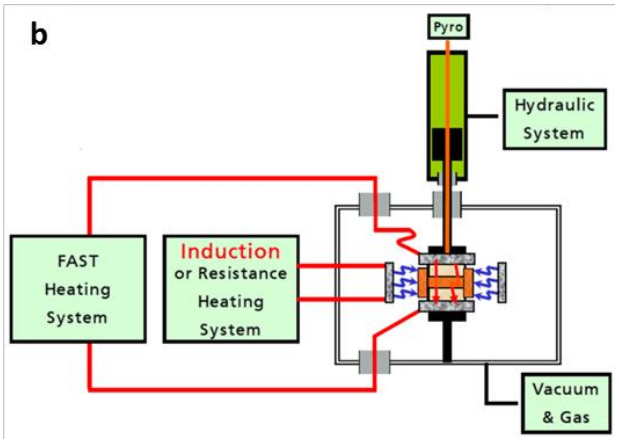

Fig. 1. Schematic of the Spark Plasma Sintering apparatus: hybrid heating (combination of SPS/FAST technology + resistance/induction heating) [17].

II. EXPERIMENTAL PROCEDURE

Commercial elemental powders Ni-Fe binary system were selected for this study. The characteristics of the raw powders are shown in Table 1. Prior to mixing, the morphology of the powders was examined with a field emission scanning electron microscopy (FESEM, JSM-7600F, Jeol, Japan) equipped with energy dispersive X-ray spectrometer (EDS). Fig. 1 (a,b) shows the SEM morphology of the eight as-received powders. SEM examination reveals an irregular Ni (Fig. 2a), while Fe (Fig. 1b) is round in shape and non-porous, typical of gas atomization produced powders. The binary powder were mixed using the Turbula Shaker Mixer T2F. An optimum mixing speed of 49 rpm and mixing time of 5h were used. A 250 ml cylindrical plastic vessel with a powder fill level of 10% was loaded axially, placed in the mixing chamber and subjected to translational and rotational motions. The mixing was carried out in a dry environment. The morphology of the mixed powders in shown in Fig. 3 with a homogenous distribution.

The mixed powders (Ni, Fe) were sintered by SPS (HHPD-25 from FCT Syteme GmbH Germany) in a 60 mm and 30 mm-inner-diameter graphite die. Graphite foils of 0.2 mm thickness were placed between the punches and the powders, and between the die and the powders for easy removal and significant reduction of temperature inhomogeneities. Sintering was performed in vacuum and a constant pressure of 30 MPa was applied from the beginning of the heating step to the end of the dwell. For all the sintering experiments, the heating was from room temperature to the desired temperature (1000°C) at the heating rate of 150°C/min. When the required temperature was reached, the electric current was shut off, the applied stress released, and the specimens were immediately cooled down in the furnace. The sintering temperature was measured by an optical pyrometer which was implanted in the SPS apparatus at 3 mm from the top of the sample surface.

Discs of 30 and 60 mm diameter of approximately 5 mm in height were produced. The 30 mm discs were produced for the purpose of optimisation and for further comparison with the 60 mm discs.

All of the sintered specimens were ground and polished to remove any surface graphite contamination. Then the sintered density was determined by the Archimedes principle. The relative density was calculated with reference to the theoretical density of the starting powders constituents using the rule of mixtures. The microstructure of specimens taken from the polished surface at cross sections (parallel to the acting force) of the sintered bodies was examined by SEM (FESEM, JSM-7600F, Jeol, Japan) incorporated with an EDX detector (Oxford X-Max) with INCA X-Stream2 pulse analyzer software, and Back Scattered Electron detectors. Focus was given on studying the microstructure at different regions along the cross section in order to avoid the influence of near-surface effects. The phases present in the sintered specimen were characterized by X-ray diffraction (XRD) using a PANalytical Empyrean model with Cu Kα radiation and analyzed using Highscore plus software. The XRD analysis was carried out on the section perpendicular to uniaxial pressed direction.

The Vickers microhardness (HV1) at room temperature were measured by a Vickers' microhardness tester (Future-tech) at a load of 100 gf and dwell time of 10s and the test result for each sample was the arithmetic mean of five successive indentations with standard deviations.

ISBN: 978-988-14048-3-1
ISSN: 2078-0958 (Print); ISSN: 2078-0966 (Online)

TABLE I.
CHARACTERISTICS OF THE RAW POWDERS USED TO PREPARE NI-50%FE.

Elemental powder	Purity (%)	Particle size (μm)	Supplier
Ni	99.5	0.5 – 3.0	WearTech
Fe	99.9	-44	WearTech

III. RESULTS AND DISCUSSION

Comparison of the sintered density for the different conditions is shown in Fig. 4. Sintered densities close to theoretical one were achieved for the 30 mm - SPS and HSPS samples, followed by the HSPS, with the least being the 60 mm – SPS sample.

The lower relative density of the 60 mm – SPS sample is not surprising due to the additional heating source in the case of HSPS which suggest uniform distribution of heat resulting in improved densification and homogeneous microstructure throughout the whole sample.

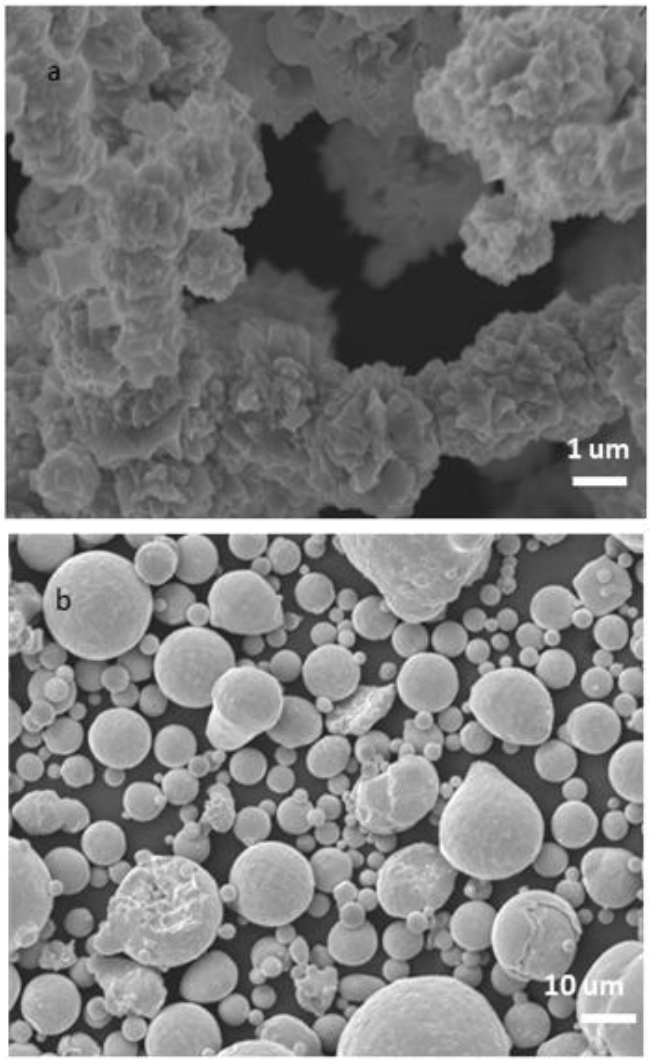

Fig. 2. SEM morphology of the as-received: (a) Ni, and (b) Fe.

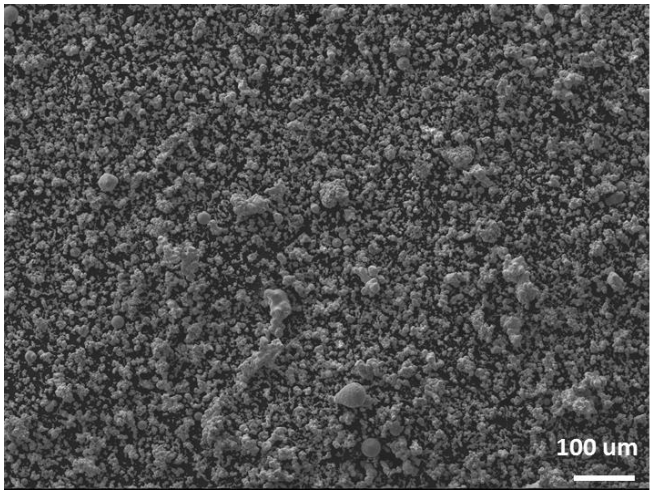

Fig. 3. SEM morphology of the mixed Ni-Fe powder.

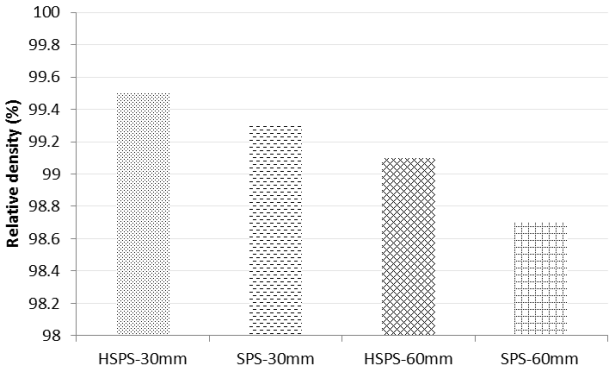

Fig. 4. Effect of sintering technique and sample diameter on the relative density Ni-Fe alloy.

The progressive evolution of microstructures in different regions of the sample manufactured using SPS and HSPS for 60 mm is given in Fig. 5. All the microstructures were taken at similar positions and low magnification (100x) in order to ensure that the grains distribution is captured. There are relatively slightly different arrangements of the grains, which respectively designate the variation in densification. It is noted that at the core of the sample for the SPS sample

(Fig. 5(a)) the microstructure is characterized by larger grains as opposed to the HSPS sample (Fig. 5(b)). During SPS of large samples there is a tendency of having a radial temperature distribution. Because of the low sintering temperature, the samples sintered via SPS had a much lower edge temperature. This suggests tremendous changes of hardness in various parts of the samples as a result of the inhomogeneous and/or varying grain size microstructure. Meanwhile, the microstructure in Fig. 5(b) has smaller grains than Fig. 5(a) indicating a better densification and more evidence of sintering necks. In SPS the high local temperature gradients enhances consolidation through thermal diffusion [18] and the higher sintering temperature, the higher overheating. With a better temperature distribution with respect to the centre of the sample (Fig 5(a), diffusion was enhanced and densification was accelerated, which resulted in increased grain size and

ISBN: 978-988-14048-3-1
ISSN: 2078-0958 (Print); ISSN: 2078-0966 (Online)

thereof better densification. The mechanical properties are expected to be greatly improved in the HSPS (Fig 5 (b and d) sample due to the homogeneous similar grain size at the core (Fig 5(b)) and edges (Fig 5(c)) of the sample. Based on this observation it is apparent that the relative density for the HSPS sample is higher than that of SPS.

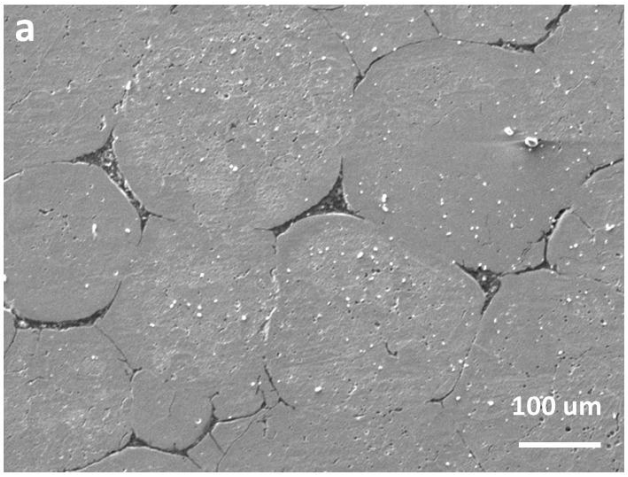

Fig. 5(a). SEM micrographs of the Ni-50%Fe alloy showing the microstructural evolution at the core of the SPS 60mm sample.

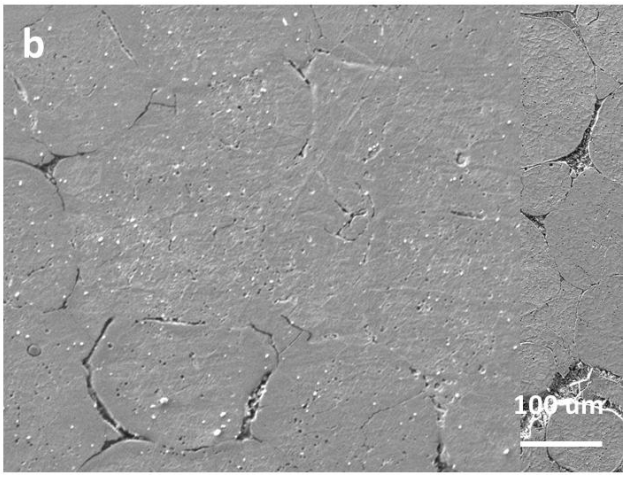

Fig. 5(b). SEM micrographs of the Ni-50%Fe alloy showing the microstructural evolution at the core of the SPS 60mm sample.

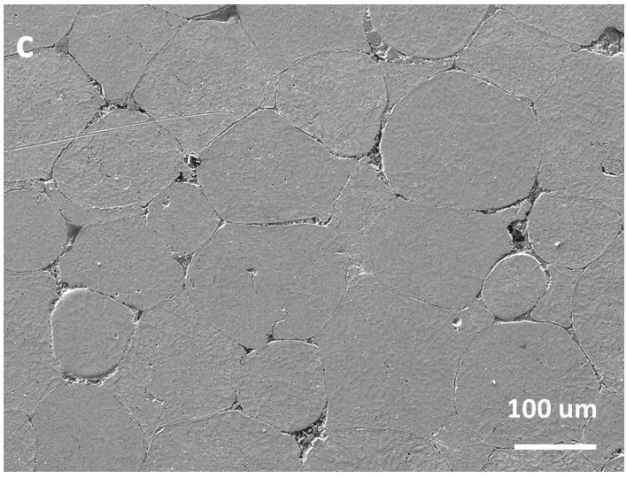

Fig. 5(c). SEM micrographs of the Ni-50%Fe alloy showing the microstructural evolution at the core of the HSPS 60mm sample.

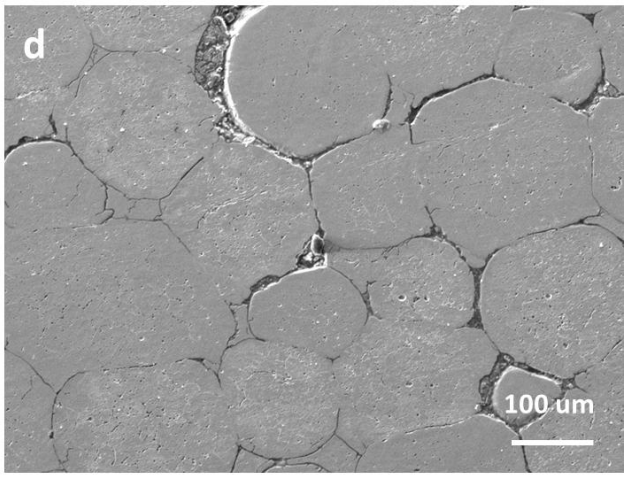

Fig. 5(d). SEM micrographs of the Ni-50%Fe alloy showing the microstructural evolution at the core of the HSPS 60mm sample.

Fig. 6 shows the micro hardness profile from edge to centre point of the sample for Ni-50%Fe fabricated by SPS and by HSPS for the 60 mm samples at 1000°C. Fig. 6 depicts the micro hardness variation on the cross-sections of the two samples. Generally, the hardness increased with increased distance from the edge. The variation in micro-hardness, which is similar to that of grain size variation from edge to the centre, is more obvious in the SPS sample. The bigger difference between the microstructure at the edge and centre especially for the SPS sample is attributed to non-uniform heat distribution resulting in poor densification at the edge and inhomogeneous microstructure that led to tremendous changes in hardness on various parts of the samples. The higher hardness at the centre of the sample relative to the edge suggest the formation of a certain amount of liquid phase which gives rise to inhomogenous microstructure. The hardness of the HSPSed material is approximately 25% higher than that of SPS at the edge of the sample, the reason being the near full densification of the former. The higher hardness values of the sample prepared by HSPS confirm that radial temperature fluctuations are minimised. Fig. 7 shows a plot of the average hardness of the samples produced by SPS and HSPS. The microhardness of HSPS and SPS sample of 60 mm and 30 mm are very close to each other, this is due to the fact for the HSPS system the 60 mm sample temperature distribution ensures good consolidation. , The good densification of the SPS 30 mm sample is as a result of the small size of the sample which allows only small radial temperature fluctuations. Compared to the HSPS 60 mm sample, the SPS 60 mm has a much smaller hardness confirming the earlier observations in Fig. 6.

ISBN: 978-988-14048-3-1
ISSN: 2078-0958 (Print); ISSN: 2078-0966 (Online)

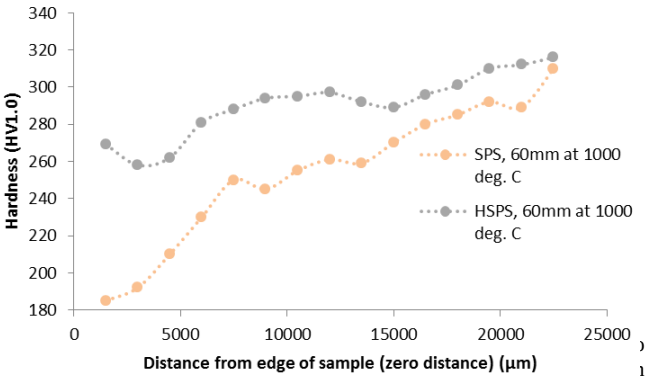

samples at 1350°C.

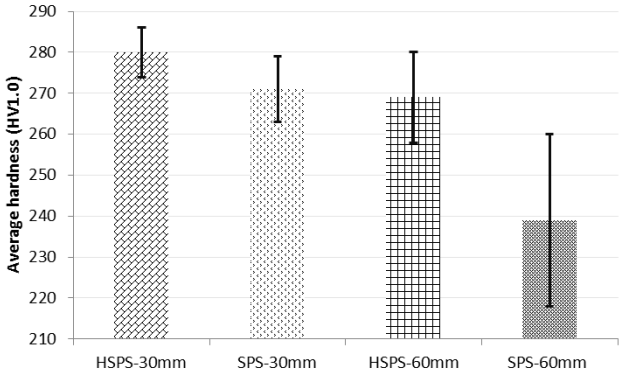

Fig. 7. Average Vickers' microhardness (HV1.0) for samples fabricated using HSPS and SPS for 30 and 60mm diameters.

IV. Conclusions

Ni-50%Fe alloys using blended powders were sintered by SPS and HSPS with 30 mm and 60 mm diameters. The microstructure and mechanical properties of the alloys were investigated. The conclusions are summarized as follows:

(1) The 60 mm-SPS sample showed a variation of grain size, while for the 60mm-HSPS minor variation were observed, confirming the minimized radial temperature fluctuations.

(2) Near full densification was achieved for the 30 mm-HSPS and SPS samples followed by 60 mm-HSPS, while the 60 mm-SPS sample had a low relative density.

(3) A micro hardness profile for the 60 mm SPS and HSPS sample was carried out, and the SPS sample had the greatest changes, even though the hardness increased for both samples towards the core of the sample. This was explained by the variation in the microstructure, as seen with changes in size and packing density, which was more obvious in the SPS sample. No variations were observed in the 30 mm samples. The average hardness values were similar for the 30 mm SPS/HSPS samples, with the 60 mm-HSPS being third highest, while the 60 mm-SPS was the least.

This work has shown that HSPS has the beneficial effect of improving or maintaining comparable properties (density and hardness) for larger samples.

Acknowledgment

This work is based on the research supported in part by the National Research Foundation of South Africa for the grant, Unique Grant No. 99348. Research facilities support by the Institute for NanoEngineering Research, Tshwane University of Technology.

References

[1] N.D. Evans, P.J. Maziasz, R.W. Swindeman, G.D. Smith, Microstructure and phase stability in Inconel alloy 740 during creep, Scr. Mater. 51 (2004) 503-507.
[2] R. Krishna, S.V. Hainsworth, H.V. Atkinson, A. Strang, Microstructural analysis of creep exposed IN617 alloy, Mater. Sci. Technol. 26 (2010) 797-802.
[3] P.S. Weitzel, A Steam Generator for 700 °C to 760 °C Advanced Ultra-Supercritical Design and Plant Arrangement: What Stays the Same and What Needs to Change, in: Proceedings of the Seventh International Conference on Advances in Materials Technology for Fossil Power Plants, Waikoloa, Hawaii, 2013.
[4] L.G. Klingensmith, in: Proceedings of the 4th Symposium on Heat Resistant Steels and Alloys for High Efficiency USC Power Plants, Beijing, China, 2011, pp. pp.307-321.
[5] P. Caron, T. Khan, Third generation superalloys for single crystal blades, in: J. Lecomte-Bechers, F. Schubert, P.J. Ennis (Eds.), Materials for Advanced Power Engineering, Forschungszentrum Jülich, Liege, Germany, 1998, pp. 897-912.
[6] C. Wang, W. Zhang, C. Ren, P. Huai, Z. Zhu, The effect of temperature on primary defect formation in Ni–Fe alloy, Nuclear Instruments and Methods in Physics Research B 321 (2014) 49–53.
[7] Groza J.R. Met. Field activation provides improved sintering. Powder Rep 2000;55:16–18.
[8] Kandukuri S. A FAST winner for fully dense nano powders. Met. Powder Rep 2008;63:22–27.
[9] Anderson K.R, Groza J.R, Fendorf M, Echer C.J. Surface oxide debonding in field assisted powder sintering. Mater. Sci. Eng. A 1999;270:278–282.
[10] Groza JR, Zavaliangos A. Sintering activation by external electrical field Mater. Sci. Eng. A 2000;287:171–177.
[11] M.B. Shongwe, M.M. Ramakokovhu, S. Diouf, M.O. Durowoju, B.A. Obadele, R. Sule, M.L. Lethabane, P.A. Olubambi Effect of starting powder particle size and heating rate on spark plasma sintering of Fe-Ni alloys, Journal of Alloys and compounds, 678 (2016) 241-248
[12] M.B. Shongwe, S. Diouf, M.O. Durowoju, P.A. Olubambi, Effect of sintering temperature on the microstructure and mechanical properties of Fe-30%Ni alloys produced by spark plasma sintering, , Journal of Alloys and compounds, 649 (2015) 824-832
[13] Ding L, Xiang DP, Li YY, Zhao YW, Li JB, Phase. Microstructure and properties evolution of fine-grained W–Mo–Ni–Fe alloy during spark plasma sintering, Materials and Design 37 (2012) 8–12.
[14] Li Y, Hu K, Li X, Ai X, Qu S. Fine-grained 93W–5.6Ni–1.4Fe heavy alloys with enhanced performance prepared by spark plasma sintering, Materials Science &Engineering A 2013;573:245–252.
[15] Upadhyaya A. Processing strategy for consolidating tungsten heavy alloys for Ordinance applications. Mater Chem Phys 2001; 67: 101–110.
[16] Humail IS, Akhtar F, Askari SJ, Jokhio MT, Qu XH, Tensile behavior change depending on the varying tungsten content of W–Ni–Fe alloys. Int. J. Refract. Met. Hard Mater 2007;25:380–385.
[17] New hybrid system on the market, http://www.fct-systeme.de/fr/news/detail/~id.9~archiv.1~page3/New-hybrid-system-on-the-market.html (accessed June 05, 2015).
[18] Olevsky EA, Froyen L. Impact of thermal diffusion on densification during SPS. J. Am. Ceram. Soc 2009;92:122-132.

ISBN: 978-988-14048-3-1
ISSN: 2078-0958 (Print); ISSN: 2078-0966 (Online)